Doping dependence of the resonance peak and incommensuration in high-T_c superconductors

Jian-Xin Li[1] and Chang-De Gong[1,2]
[1]*National Laboratory of Solid States of Microstructure and Department of Physics, Nanjing University, Nanjing 210093, China*
[2]*Chinese Center of Advanced Science and Technology (World Laboratory), P.O. Box 8730, Beijing 100080, China*
(Received 22 March 2001; revised manuscript received 8 April 2002; published 24 June 2002)

The doping and frequency evolutions of the incommensurate spin response and the resonance mode in the superconducting state of high-T_c cuprates are studied based on the scenario of the Fermi-surface topology. We use the slave-boson mean-field approach to the t-t'-J model and include the antiferromagnetic fluctuation correction in the random-phase approximation. We find that the equality between the incommensurability and the hole concentration is reproduced at low frequencies in the underdoped regime. We also obtain the downward dispersion for the spin response and predict its doping dependence for further experimental testing, as well as a proportionality between the low-energy incommensurability and the resonance energy. Our results suggest a common origin for the incommensuration and the resonance peak based on the Fermi-surface topology and the *d*-wave symmetry.

DOI: 10.1103/PhysRevB.66.014506 PACS number(s): 74.72.−h, 74.25.Ha, 75.40.Gb

The inelastic neutron-scattering experiment plays an important role in the studies of the spin dynamics in high-T_c superconductors. It can provide the momentum and frequency dependences of the dynamical spin susceptibility. Over the past decade, the striking feature of the spin susceptibility observed in the momentum space is the incommensurate peak along the $(\pi,\pi+\delta\pi)$ direction,[1–3] and that in the frequency dependence is the resonance peak at the antiferromagnetic (AF) wave vector $\mathbf{Q}=(\pi,\pi)$.[4,5] These stimulate intensive experimental and theoretical studies. Recently, it is suggested that the presence of dynamic stripes is the origin of the observed incommensurate peak, at least for $La_{2-x}Sr_xCuO_4$.[6] One of its strong supports comes from the experiment by Yamada *et al.*[2] that shows an equality between the incommensurability and the doping concentration (Yamada plot) in the superconducting (SC) state of the underdoped $La_{2-x}Sr_xCuO_4$. This equality follows naturally from the static stripe model, but has not been explained in any other way up to now.[7] However, it is now unclear how to explain the resonance peak based on this scenario. On the other hand, the gross features of the incommensurate spin fluctuations can also be explained based on the scenario of the nested Fermi surface[8–10] (FS) and the resonance peak is thought to be a collective spin excitation mode in this framework.[8,11] Obviously, more fine and detailed experimental data are helpful for selecting out or ruling out the above models. In addition to the Yamada plot, we note that some other experimental developments have also been reported. Among these are the detailed evolutions of the resonance peak and incommensurability with doping,[12,13] and the dispersion connecting these two structures that has a downward curvature opposite in sign to a conventional magnon dispersion.[14,15]

In view of these experimental observations, we present in this paper a detailed investigation of the doping and frequency dependences of the incommensurability and the resonance peak energy, and their relationship based on the nested Fermi-surface scenario. We start from the slave-boson mean-field theory of the two-dimensional (2D) t-t'-J model and include the AF spin fluctuations by random-phase approximation (RPA). The aim of choosing this approach is that we can incorporate the evolutions of the FS and the SC gap with dopings self-consistently at the mean-field level and determine their values according to the well accepted input parameters t,t',J. This enables us to carry out a quantitative study of the doping and frequency evolutions of spin fluctuations. In previous studies,[9,11,16] a tight-binding dispersion and the magnitude of the SC gap that are inferred from related experimental data for a fixed doping concentration are taken phenomenologically. Consequently, these investigations are limited to a fixed hole doping. There are also investigations[17] that start from the mean-field theory of the t-t'-J model, but they ascribe the origin of the incommensurate peak to the spiral spin-density waves, not to the Fermi-surface topology. Moreover, Batista *et al.*[17] used the slave-fermion approach that produces a small pocket-like Fermi surface and, therefore, is only suitable for very low dopings. The approach adopted here has also been used before to investigate the spin response in high-T_c cuprates and is shown to reproduce the experimental data at that time.[8,18] The main results we obtain in this paper are as follows.

(1) We find that the equality between the low-energy incommensurability and doping density in the SC state of the underdoped regime is reproduced. This may provide an alternative to its exclusive stripe-phase explanation.

(2) The doping dependence of the downward dispersion of the collective mode is investigated. We find that the reemergence of the incommensurate peak above the resonance frequency is strongly doping dependent. It is along the $(\pi,\pi+\delta\pi)$ direction in the underdoped regime ($x\leqslant 0.13$) and along the diagonal direction in the optimally doped and overdoped regimes $x\geqslant 0.14$. The crossover frequency at which the incommensurate peak shifts from the $(\pi,\pi+\delta\pi)$ direction to the diagonal direction due to the node-to-node excitations as previously reported[8,19] increases with doping.

(3) The resonance energy has a linear relation with doping in the underdoped regime and saturates near optimal doping,

then slightly decreases with doping in the overdoped regime. As a result, a proportionality between the low-energy incommensurability and the resonance energy is obtained.

We note that a similar equality between the incommensurability and the doping density was obtained previously in the normal state,[20] instead of the SC state described here. In the SC state, the RPA correction factor strongly affects the position of the incommensurate vectors due to the steplike rise in the imaginary part of the bare spin susceptibility at the spin excitation gap edge, as will be described below. The downward dispersion of the collective mode has also been studied by Norman[16] and Chubukov *et al.*[21] very recently. Their investigations are based on the phenomenological model as discussed above, so no doping dependence is presented. The reemergence of the incommensuration above the resonance frequency has been discussed in Ref. 10. Compared with the result at a fixed doping density in Ref. 10, we find that the reemergent incommensurate peaks have different orientation in the momentum space in the underdoped and overdoped regimes. This may act as one of the testing observations for the applicability of the present approach. Most of the results reported here are consistent with experimental data[13,22] and the others wait for further experimental testing. Therefore, our result presents an alternative explanation of the incommensuration and resonance peak in the spin response based on the *d*-wave superconductor with tight-binding dispersion. However, the abrupt saturation of the incommensurability near the optimal doping and in the overdoped regime that is observed both in $La_{2-x}Sr_xCuO_4$ (Ref. 2) and $YBa_2Cu_3O_{6+x}$ (Ref. 13) is not found. Possible reason for this is discussed.

In the slave-boson approach to the t-t'-J model,[8,23] the physical electron operators $c_{i\sigma}$ are expressed by slave bosons b_i carrying the charge and fermions $f_{i\sigma}$ representing the spin; $c_{i\sigma}=b_i^+ f_{i\sigma}$. In this paper, we will focus on the spin dynamics in the SC state. In this case, we consider the order parameters $\Delta_{ij}=\langle f_{i\uparrow}f_{j\downarrow}-f_{i\downarrow}f_{j\uparrow}\rangle=\pm\Delta_0$ with the *d*-wave symmetry and $\chi_{ij}=\Sigma_\sigma\langle f_{i\sigma}^+ f_{j\sigma}\rangle=\chi_0$, in which bosons condense $b_i\rightarrow\langle b_i\rangle=\sqrt{x}$ (x is the hole concentration). Then, the slave-boson mean-field Hamiltonian of the 2D t-t'-J model in the SC state is,

$$H_m=\sum_{k\sigma}\epsilon_k f_{k\sigma}^\dagger f_{k\sigma}-\sum_k \Delta_k(f_{k\uparrow}^\dagger f_{-k\downarrow}^\dagger+\text{H.c.}) + 2NJ'(\chi_0^2+\Delta_0^2), \tag{1}$$

where $\epsilon_k=-2(xt+J'\chi_0)[\cos(k_x)+\cos(k_y)] -4xt'\cos(k_x)\cos(k_y)-\mu$ is the dispersion for fermions, and $\Delta_k=2J'\Delta_0[\cos(k_x)-\cos(k_y)]$, with $J'=3J/8$. The normal-state Fermi surface at doping $x=0.12$ for this dispersion is shown in Fig. 1. The mean-field parameters χ_0, Δ_0, and the chemical potential μ for different dopings are obtained from a self-consistent calculation.[23]

It has been shown[8,24,25] that the inclusion of the AF fluctuation correction is necessary to account for some of the spin and charge dynamics. Formally, this can be done by perturbing around the mean-field Hamiltonian, i.e., we write

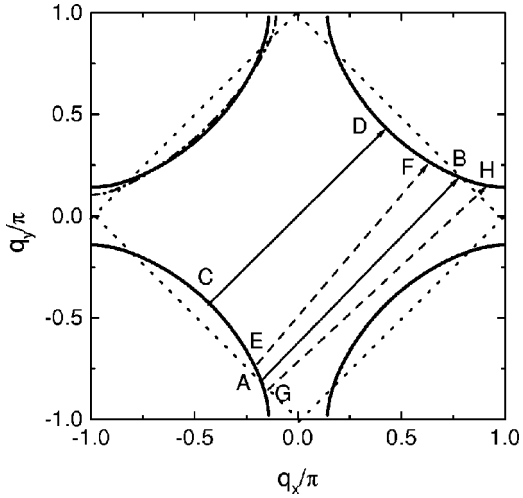

FIG. 1. Fermi surface for the dispersion ϵ_k (thick solid line) at hole doping $x=0.12$. The thin solid and dashed lines with arrows denote the threshold particle-hole excitations for different wave vectors (see text). For a comparison, that part of the Fermi surface for $t/t'=-0.35$ in the second quadrant at the same doping is shown as the dotted-dashed line.

$H=H_m+H'$ with H the usual 2D t-t'-J Hamiltonian, and treat H' as a perturbation. In principle, all fluctuations are included. However, different selection of subset diagrams may result in different kinds of fluctuations. For the spin fluctuation, the usual RPA approach selects a series of ring diagrams as shown in Refs. 8,24 and 25. Then, the renormalized spin susceptibility is given by

$$\chi(\mathbf{q},\omega)=\frac{\chi_0(\mathbf{q},\omega)}{1+\eta J\gamma_q\chi_0(\mathbf{q},\omega)}, \tag{2}$$

where $\gamma_q=\cos(q_x)+\cos(q_y)$. χ_0 is the bare spin susceptibility that comes from the fermionic bubble and is given by the usual BCS form.[26] As done before,[8,24,25] we choose $\eta=0.34$ instead of $\eta=1$, in order to set the AF instability at $x=0.02$ that is the experimental observed value for $La_{2-x}Sr_xCuO_4$.[27]

Numerical calculations are performed by dividing the Brillouin zone into 1024×1024 lattices, with $t=2J, t'=-0.45t$, and $J=0.13$ eV. The damping rate of the fermionic quasiparticles is stimulated to be $\Gamma=0.004J$, however, we note that the incommensurability and the resonance energy is not subjected to the change of Γ when it is below $0.1J$.

Before presenting our results, it is important to point out that the bare spin susceptibility $\text{Im}\chi_0$ is *incommensurate* for all energies and dopings in the ranges considered here. Moreover, its peak is along the $(\pi+\delta\pi,\pi)$ or $(\pi,\pi+\delta\pi)$ directions. It comes from the FS nesting effect as has been shown by Brinckmann and Lee.[8] In Fig. 2, the peak position of the imaginary part of the renormailized spin susceptibility is shown as a function of frequency, for doping concentrations $x=0.08$,0.14, and 0.20, which may correspond to the underdoped, optimally doped, and overdoped regimes. At their

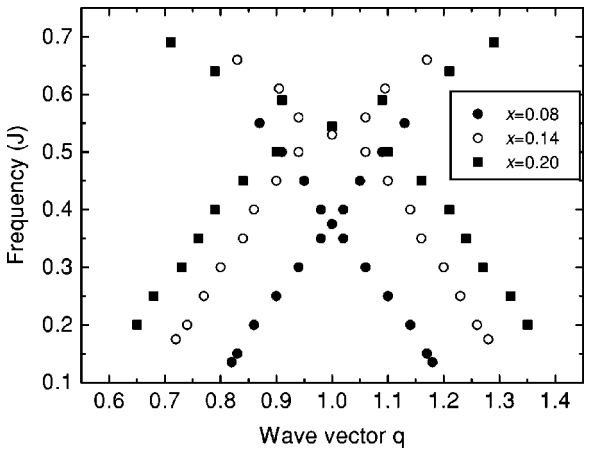

FIG. 2. Peak positions of the imaginary part of the renormalized spin susceptibility in the q space as a function of frequency for doping concentrations $x=0.08$, 0.14, and 0.20. In the downward dispersion range, the incommensurate peaks are along the $(\pi,\pi+\delta\pi)$ direction, so the horizontal axis is in unit of $(1,q)\pi$. Below $\omega=0.135J$, $0.175J$, and $0.2J$ at dopings $x=0.08$, 0.14, and 0.20, respectively, and for frequencies above the resonance energy at $x=0.14$ and 0.20, they are along the diagonal direction. In the latter case, the horizontal axis is in unit of $(q,q)\pi$.

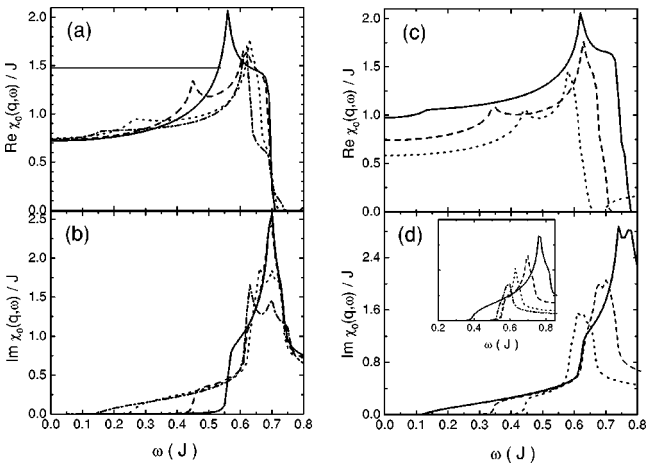

FIG. 3. Frequency dependence of the bare spin susceptibility χ_0. (a) and (b) are the real and imaginary parts of the bare spin susceptibility at doping $x=0.14$ for different $\mathbf{q}$. The solid line, the dashed-dotted line, the dotted line, and the dashed line denote spin susceptibilities at $\mathbf{q}=(\pi,\pi),(\pi,0.72\pi),(\pi,0.8\pi)$, and $(\pi,0.9\pi)$, respectively. The thin line in (a) denotes $-1/2\eta J$, so its cross with the real part corresponds to the pole of the renormalized spin susceptibility. (c) and (d) are the real and imaginary parts of the bare spin susceptibility at $\mathbf{q}=(\pi,0.84\pi)$ for different dopings. The solid line, dashed line, and dotted line denote spin susceptibility at $x=0.08$, 0.14, and 0.2, respectively. The inset of (d) shows the frequency dependence of $\mathrm{Im}\chi_0$ at $\mathbf{q}=(\pi,\pi)$ for the doping $x=0.08$ (solid line), 0.14 (dashed line), 0.20 (dotted line), and 0.24 (dashed-dotted line).

resonance energies ($0.375J$, $0.53J$, and $0.545J$, respectively), the q peaks are at $\delta=0$, i.e., at (π,π) point. When the frequency is reduced from the resonance energy, the incommensurate peak occurs and is found to be in the $(\pi,\pi+\delta\pi)$ direction. In particular, a downward curvature for the peak dispersion is observed for various dopings. This is in agreement with experiments.[14,15] To understand its origin, we show the frequency dependences of the bare spin susceptiblity $\mathrm{Im}\chi_0$ at $x=0.14$ for different wave vectors $\mathbf{q}=(\pi,0.72\pi),(\pi,0.8\pi)$, and $(\pi,0.9\pi)$ in Figs. 3(a) and 3(b), and at $\mathbf{q}=(\pi,0.84\pi)$ for different dopings $x=0.08$, 0.14, and 0.20 in Figs. 3(c) and 3(d). In the current framework, the origin of the resonance peak is ascribed to a collective spin excitation mode corresponding to the pole of the renormalized spin susceptibility, i.e., $1+\eta J\gamma_{\mathbf{Q}}\mathrm{Re}\chi_0(\mathbf{Q},\omega)=0$, and negligibly small $\mathrm{Im}\chi_0(\mathbf{Q},\omega)$.[8,11,24] At the commensurate wave vector $\mathbf{Q}=(\pi,\pi)$, there is a steplike rise in $\mathrm{Im}\chi_0$ [shown as the soild line in Fig. 3(b)] at the threshold energy for particle-hole (p-h) excitations. Due to this steplike rise, a logarithmic singularity in $\mathrm{Re}\chi_0$ occurs via the Kramers-Kroenig relation. This singularity shifts downward the collective-mode energy and leads it to situate in the spin gap, so no damping is expected for the mode. For the energy band ϵ_k and the SC gap considered here, the initial and final states of the p-h excitations at the threshold energy (minmum excitation energy) lie on the Fermi surface. So, the threshold excitation with transition wave vector $\mathbf{Q}$ corresponds to the excitation $A\rightarrow B$ as schematically shown in Fig. 1. The steplike rise is caused mainly by the van Hove (vH) singularity around $(\pi,0)$ and the d-wave symmetry of the SC gap.[11,24,25] In this case, the collective spin excitation mode at (π,π) that is determined by the pole condition in the RPA correction $(1+\eta J\gamma_q\chi_0)^{-1}$ dominates the structure of the renormalized spin susceptibility $\mathrm{Im}\chi$ and shows up as a strong commensurate resonance peak, although the bare spin susceptibility $\mathrm{Im}\chi_0$ is incommensurate. When the wave vector $\mathbf{q}$ moves away from $\mathbf{Q}$, the p-h transitions will move to the node direction and that connecting $(0,\pi)$ and $(\pi,0)$, respectively. As a result, the single steplike rise splits into two as shown in Fig. 3(b). One is at the energy below it and another above it, which correspond to the excitations $E\rightarrow F$ and $G\rightarrow H$ as in Fig. 1, respectively. The pole equation still satisfies around the high-energy peak (The line denoting $-1/\eta J\gamma_q$ for $\mathbf{q}\neq\mathbf{Q}$ will rise above the thin line in Fig. 3(a) due to $|\gamma_q|<|\gamma_Q|$), but the pole position falls well above the gap and the resultant p-h excitations are overdamped, so it does not affect the structure of the spin excitations. On the other hand, though the peak caused by the low-energy jump does not satisfy the pole equation, because its jump height is reduced due to the weakening of the vH singularity at the $\mathbf{q}$ points E and F, which are away from $(0,-\pi)$ and $(\pi,0)$, it will show up in the spin response via the RPA correction, because of the small damping of the excitations. We can see from Fig. 3(b) that, when the deviation of the wave vector $\mathbf{q}$ from $\mathbf{Q}$ increases, the energy of the corresponding low-energy jump decreases. From Ref. 8, we also know that the incommensurability of $\mathrm{Im}\chi_0$ increases with the decrease of frequency. So, the peak dispersion determined both from the RPA correction and the bare spin susceptibility $\mathrm{Im}\chi_0$ has a downward curvature. But, which one mainly determines the position of the incommensurate peak in the renormalized spin susceptibility is interesting. This issue is related to the argument that attributes the incommensurate magnetic re-

sponse and the commensurate resonance belongs to parts of the same collective mode.[15,29] In the previous investigation,[8] the incommensurate magnetic response is explained solely based on the structure of $\mathrm{Im}\chi_0$, because of the consideration $\chi \approx \chi_0$. However, we find that the peak position of $\mathrm{Im}\chi$ in q space, i.e., the incommensurability, is mainly determined by the RPA correction $1+\eta J \gamma_q \chi_0$ and in turn by the low-energy steplike rise. This can be seen clearly from Fig. 3(b), where the dashed-dotted line, the dotted line, and the dashed line denote the imaginary parts of the bare spin susceptibility $\mathrm{Im}\chi_0$ at $\mathbf{q}=(\pi,0.72\pi)$,$(\pi,0.8\pi)$, and $(\pi,0.9\pi)$, respectively. These wave vectors are the incommensurate peak positions in the renormalized spin susceptibility $\mathrm{Im}\chi$ at frequencies $\omega=0.15J$,$0.3J$, and $0.45J$, respectively. Clearly, the low energy steplike rises in $\mathrm{Im}\chi_0$ as shown in Fig. 3(b), and consequently the low-energy peaks in their real parts shown in Fig. 3(a) are at the same values as the above frequencies for the corresponding wave vectors. On the other hand, the incommensurabilities in $\mathrm{Im}\chi_0$ for $\omega=0.15J$, $0.3J$, and $0.45J$ are at $\mathbf{q}=(\pi,0.72\pi)$,$(\pi,0.76\pi)$, and $(\pi,0.88\pi)$. The same situation is found for other doping concentrations. Therefore, both the resonance peak and the incommensurability are mainly determined by the steplike rise of $\mathrm{Im}\chi_0$.

Below the lowest frequency for each doping density shown in Fig. 2, we find that a crossover of the incommensurate peaks from the $(\pi,\pi+\delta\pi)$ direction to the diagonal direction occurs. It is because the excitations will be limited to be along the diagonal direction (the node-to-node excitation), such as $C \rightarrow D$ as shown in Fig. 1, when the excitation energy is below the crossover energy due to the energy-conservation law and the *d*-wave symmetry of the SC gap. It is a specular feature for the model based on the FS topology and may also act to distinguish between the stripe and the FS nesting models. Unfortunately, the crossover energy for the underdoped system is too low to be available for the experimental observation due to the dim scattering intensity.[13] However, we can see from Fig. 2, that it increases with doping density and is about $0.135J$, $0.175J$, and $0.2J$ for the doping $x=0.08$, 0.14, and 0.20, respectively. So, we expect that it may be in the experimental observable range for the overdoped cuprates. For example, the crossover energy for $x=0.20$ is $0.2J \approx 26$ meV, which is experimentally accessible according to the recent paper.[13] Above the resonance frequency, the incommensurate peak occurs again. In particular, we find that only in the underdoped regime ($x \leqslant 0.13$) are the incommensurate peaks along the $(\pi,\pi+\delta\pi)$ direction. They are along the diagonal direction in the optimally doped and overdoped regimes ($x \geqslant 0.14$). It in fact reflects the doping dependence of the intensity ratio of the incommensurate peak along the $(\pi,\pi+\delta\pi)$ direction to that along the diagonal direction, which decreases with the increase of doping density when the frequency is above the resonance energy.[28] From Fig. 2, one can see that the incommensurability above the resonance frequency increases with frequency, so the dispersion shows a upward curvature that is similar to that of a massive magnon in a disorder Néel state.

We show the doping dependences of the incommensurability δ in the $(\pi,\pi+\delta\pi)$ direction in Fig. 4(a), for energies

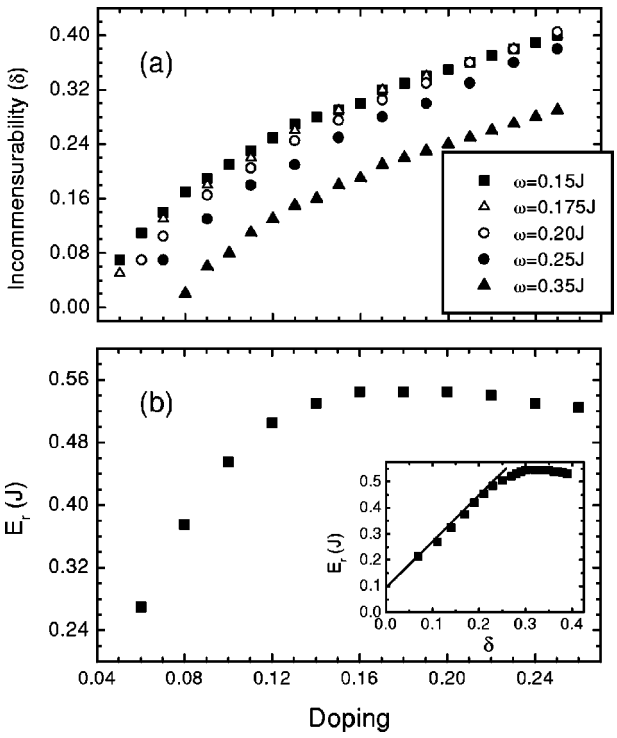

FIG. 4. (a) Doping dependences of the incommensurability δ in the $(\pi,\pi+\delta\pi)$ direction for different frequencies. (b) Doping dependence of the resonance energy E_r. The inset of (b) shows the ratio between the incommensurability and the resonance energy. The solid line in the inset is a guide to the eye. Note that the incommensurability δ defined here is twice that used by experimentists that is indexed in units of the reciproal-lattice vectors.

$\omega=0.15J$, $0.175J$, $0.20J$, $0.25J$, and $0.35J$. In the underdoped regime, the incommensurability increases with the increase of doping and exhibits a nearly linear doping dependence for all energies. In the high-energy range, the incommensurability increases with the decrease of frequency. For $La_{2-x}Sr_xCuO_4$, it is found that the incommensurability is energy independent for $\hbar\omega<15$ meV. The same behavior is found here when the frequency is reduced to be below about $\omega=0.20J$, as can be seen from Fig. 4(a). By a closer inspection of the doping dependence of the incommensurability at low frequencies such as $\omega=0.175J$ and $0.15J$, we find that the equality $\delta=2x$ holds in the doping range from $x=0.06$ to $x=0.13$. We note that the incommensurability δ defined here is twice that used by experimentalists that is indexed in units of the reciproal-lattice vectors. This equality has been observed at low frequencies in underdoped cuprates[2,13] and is believed to be explained previously by the stripe model.[7] Therefore, our result provides an alternative explanation based on the FS nesting. However, the incommensurability increases continually in the whole doping range, which is different from the experimental observation that it saturates near the optimal doping and in the overdoped regime.[2,13] We also show the doping dependences of the resonance energy E_r in Fig. 4(b). This result has been reported by Li and his co-workers in a smaller doping range before.[24] A nearly linear doping dependence of the resonant

energy E_r is found in the underdoped regime, then it saturates in the slightly overdoped regime and eventually decreases with the further increase of dopings. Due to the similar doping dependence in the underdoped regime, the ratio of E_r to δ shows a linear behavior as can be seen in the inset of Fig. 4(b). These results are remarkably in agreement with experiments.[13,22] To understand these behaviors, we show the frequency dependences of the bare spin susceptibility χ_0 at the incommensurate **q** point $(\pi,0.84\pi)$ for different dopings as shown in Figs. 3(c) and 3(d), and at the commensurate **q** point (π,π) in the inset of Fig. 3(d). We find that the steplike rise at (π,π) and the low-energy steplike rise at $(\pi,0.84\pi)$ increases monotonously with doping in the underdoped regime. But the former saturates in the optimally doped regime and then decreases with the further increase of dopings, and the latter increases with dopings in the whole doping range considered here. According to the above discussion, it is this feature that leads to the special doping dependences for both cases. From this reasoning, we may also argue that the saturation of the incommensurability observed experimentally near and after the optimal doping should not be related *only* to the change of the FS topology. Whether new physics such as the stripe phase is required or some additional factors such as the change of the quasiparticle nature due to a quantum critical point near the optimal doping[30] should be taken into consideration, is an open question.

The equality of the incommensurability and the doping density at low energies presented above is obtained using a set of fixed parameters ($t/J=2, t'/t=-0.45$, and $\eta=0.34$), which has been used in the previous studies[8,24,25] and shown to be able to describe many properties in high-T_c cuprates. However, there is a variation between the onset doping densities for the AF instability among different cuprates.[27] To see its effect, we have carried out the calculations with $\eta=0.426$ that corresponds to setting the AF instability at $x_c=0.05$.[31] The results are presented in Fig. 5(a), together with those for $\eta=0.34$. From a comparison, we can see that the increase of η will lead to a decrease of the incommensurability and this change will decrease with the reduction of frequency. When frequency is reduced to be near $\omega=0.15J$, no obvious difference between the results obtained with $\eta=0.34$ and $\eta=0.426$ is observed. It is due to the weakness of the RPA correction factor $(1+\eta J\gamma_q \mathrm{Re}\chi_0)^{-1}$ in the determination of the momentum structure of the renormalized spin susceptibility when frequency is low, because the p-h excitations with decreasing frequency will move towards the node area that is more away from those excitations $A\rightarrow B$ (indicated in Fig. 1), which satisfy the pole condition. Another discussion of the robustness of the equality is how it depends on the parameters t'. We show in Fig. 5(b) a comparison of the results using $t'/t=-0.35,-0.40$, and -0.55 with that using $t'/t=-0.45$. When $|t'/t|$ decreases, the FS will be less, and less curved as can be seen from Fig. 1, where the dotted-dashed line in the second quadrant denotes a part of the FS for $t'/t=-0.35$. In particular, the FS near the nodes will move towards the $(\pm\pi/2,\pm\pi/2)$ points. As a result, the incommensurability will decrease with $|t'/t|$ at a fixed frequency. However, this change becomes less and less

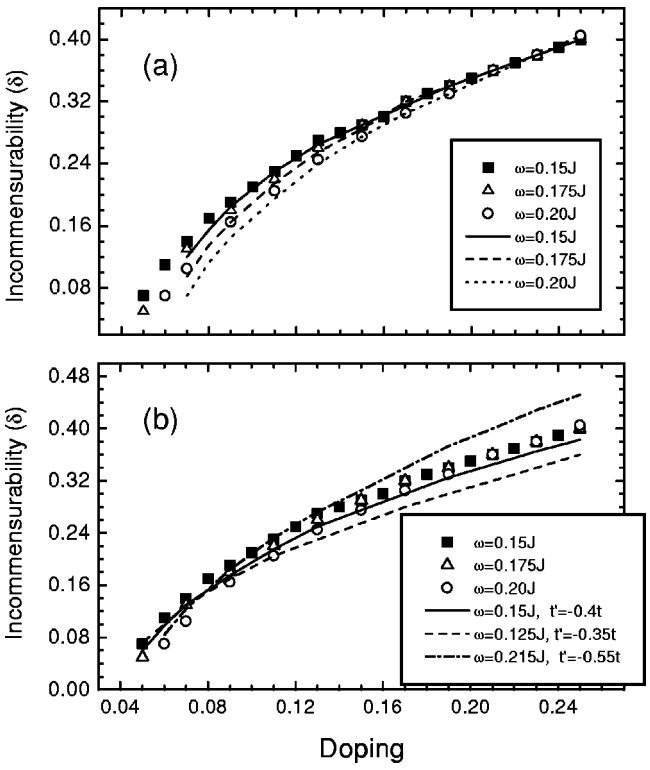

FIG. 5. (a) Comparison of the doping dependences of the incommensurability δ in the $(\pi,\pi+\delta\pi)$ direction for $\eta=0.34$ (scattered points) and $\eta=0.426$ (lines). (b) Comparison of the doping dependences of the incommensurability δ in the $(\pi,\pi+\delta\pi)$ direction for $t/t'=-0.45$ (scattered points), $t/t'=-0.35$ (dashed line), $t/t'=-0.40$ (solid line), and $t/t'=-0.55$ (dotted-dashed line).

obvious when the doping concentration is reduced. So, in the doping range from $x=0.06$ to 0.10 the equality still holds for $\omega=0.125J$, $0.15J$, and $0.215J$ in the cases of $t'/t=-0.35$, -0.45, and -0.55, respectively. This indicates that the incommensurability is sensitive to the FS topology, but this sensitivity drops when the doping density is decreased. Therefore, the equality between the incommensurability and the doping concentration can survive a certain range of change in t', because it holds at low dopings. From above discussions, we may conclude that our result of the equality of the incommensurability and the doping density at low energies is robust.

In summary, we have examined the doping and frequency dependences of the incommensurability and the resonance energy in the SC state of high-T_c cuprates based on the Fermi-surface topology. The calculations are carried out by use of the slave-boson mean-field approach to the t-t'-J model and including the antiferromagnetic fluctuation correction in the random-phase approximation. We find that the equality of the incommensurability and the doping density exists at lower frequencies in the underdoped regime. The downward dispersion is reproduced and its doping dependence is presented for further experimental testing. We also find a good linear behavior between the incommensurability and the resonance energy in the underdoped regime, which

is consistent with experiments. Our results may suggest a common origin for the incommensurate spin response and the resonance peak based on the Fermi-surface topology and the *d*-wave superconductivity.

J.X.L thanks T. K. Lee for useful conversations. He was supported by the National Nature Science Foundation of China. C.D.G. thanks the support by the Ministry of Science and Technology of China (NKBRSF-G19990646).

[1] T.E. Mason, G. Aeppli, and H.A. Mook, Phys. Rev. Lett. **68**, 1414 (1992).
[2] K. Yamada, C.H. Lee, K. Kurahashi, J. Wada, S. Wakimoto, S. Ueki, H. Kimura, Y. Endoh, S. Hosoya, G. Shirane, R.J. Birgeneau, M. Greven, M.A. Kaster, and Y.J. Kim, Phys. Rev. B **57**, 6165 (1998).
[3] B. Lake, G. Aeppli, T.E. Mason, A. Schroder, D.F. McMorrow, K. Lefmann, M. Isshiki, M. Nohara, H. Takagi, and S.M. Hayden, Nature (London) **400**, 43 (1999).
[4] J. Rossat-Mignod, L.P. Regnault, C. Vettier, P. Bourges, P. Burlet, J. Bossy, J.Y. Henry, and G. Lapertot, Physica C **185-189**, 86 (1991).
[5] H.F. Fong, B. Keimer, P.W. Anderson, D. Reznik, F. Doğan, and I.A. Aksay, Phys. Rev. Lett. **75**, 316 (1995).
[6] J.M. Tranquada, B.J. Sternlieb, J.D. Axe, Y. Nakamura, and S. Uchida, Nature (London) **375**, 561 (1995); J.M. Tranquada, J.D. Axe, N. Ichikawa, Y. Nakamura, S. Uchida, and B. Nachumi, Phys. Rev. B **54**, 7489 (1996).
[7] J. Orenstein and A.J. Millis, Science **288**, 468 (2000). We note that a similar equality was obtained in the normal state before, see Ref. 20.
[8] J. Brinckmann and P.A. Lee, Phys. Rev. Lett. **82**, 2915 (1999).
[9] K.K. Voo, W.C. Wu, J.X. Li, and T.K. Lee, Phys. Rev. B **61**, 9095 (2000); D.K. Morr and D. Pines, *ibid.* **61**, 6483 (2000).
[10] Y.J. Kao, Q. Si, and K. Levin, Phys. Rev. B **61**, 11 898 (2000).
[11] G. Blumberg, B.P. Stojkovic, and M.V. Klein, Phys. Rev. B **52**, 15 741 (1995); D.Z. Liu, Y. Zha, and K. Levin, Phys. Rev. Lett. **75**, 4130 (1995); J.X. Li, W.G. Yin, and C.D. Gong, Phys. Rev. B **58**, 2895 (1998).
[12] H.F. Fong, P. Bourges, Y. Sidis, L.P. Regnault, J. Bossy, A. Ivanov, D.L. Milius, I.A. Aksay, and B. Keimer, Phys. Rev. B **61**, 14 773 (2000).
[13] P. Dai, H.A. Mook, R.D. Hunt, and F. Doǵan, Phys. Rev. B **63**, 054525 (2001).
[14] M. Arai, T. Nishijima, Y. Endoh, T. Egami, S. Tajima, K. Tomimoto, Y. Shiohara, M. Takahashi, A. Garret, and S.M. Bennington, Phys. Rev. Lett. **83**, 608 (1999).
[15] P. Bourges, Y. Sidis, H.F. Fong, L.P. Regnault, J. Bossy, A. Ivanov, and B. Keimer, Science **288**, 1234 (2000).
[16] M.R. Norman, Phys. Rev. B **63**, 092509 (2001).
[17] M. Deeg and H. Fehske, Phys. Rev. B **50**, 17 874 (1994); C.D. Batista, L.O. Manuel, H.A. Ceccatto, and A.A. Aligia, Europhys. Lett. **38**, 147 (1997).
[18] T. Tanamoto, K. Kuboki, and H. Fukuyama, J. Phys. Soc. Jpn. **60**, 3072 (1991).
[19] J.P. Lu, Phys. Rev. Lett. **68**, 125 (1992).
[20] Q. Si, Y. Zha, K. Levin, and J.P. Lu, Phys. Rev. B **47**, 9055 (1993).
[21] A.V. Chubukov, B. Janko, and O. Tchernyshyov, Phys. Rev. B **63**, 180507 (2001).
[22] H. He, Y. Sidis, P. Bourges, G.D. Gu, A. Ivanov, N. Koshizuka, B. Liang, C.T. Lin, L.P. Regnault, E. Schoenherr, and B. Keimer, Phys. Rev. Lett. **86**, 1610 (2001).
[23] M.U. Ubbens and P.A. Lee, Phys. Rev. B **46**, 8434 (1992).
[24] J.X. Li, C.Y. Mou, and T.K. Lee, Phys. Rev. B **62**, 640 (2000).
[25] J.X. Li, C.Y. Mou, C.D. Gong, and T.K. Lee, Phys. Rev. B **64**, 104518 (2001).
[26] J.R. Schriffer, *Theory of Superconductivity* (Benjamin, Massachusetts, 1964).
[27] A.P. Kampf, Phys. Rep. **249**, 219 (1994).
[28] We note that this intensity ratio nearly does not change with the variation of dopings in the downward dispersion range.
[29] C.D. Batista, G. Ortiz, and A.V. Balatsky, cond-mat/0008345 (unpublished).
[30] S. Sachdev, Science **288**, 5465 (2000).
[31] According to Ref. 27, the AF instability in $La_{2-x}Sr_xCuO_4$ is at $x_c=0.02$ and in $YBa_2Cu_3O_{6+\delta}$ is near $\delta=0.42$. Though the corresponding hole concentration for $YBa_2Cu_3O_{6+\delta}$ is expected to be larger than x_c, we cannot determine it exactly because there is no one to one correspondence between δ and x.